



HAL
open science

A multi well-balanced scheme for the shallow water MHD system with topography

François Bouchut, Xavier Lhébrard

► **To cite this version:**

François Bouchut, Xavier Lhébrard. A multi well-balanced scheme for the shallow water MHD system with topography. 2015. hal-01131297v1

HAL Id: hal-01131297

<https://hal.science/hal-01131297v1>

Preprint submitted on 13 Mar 2015 (v1), last revised 1 Dec 2016 (v3)

HAL is a multi-disciplinary open access archive for the deposit and dissemination of scientific research documents, whether they are published or not. The documents may come from teaching and research institutions in France or abroad, or from public or private research centers.

L'archive ouverte pluridisciplinaire **HAL**, est destinée au dépôt et à la diffusion de documents scientifiques de niveau recherche, publiés ou non, émanant des établissements d'enseignement et de recherche français ou étrangers, des laboratoires publics ou privés.

A multi well-balanced scheme for the shallow water MHD system with topography

François Bouchut*, Xavier Lhébrard*

Abstract

The shallow water magnetohydrodynamic system involves different families of physically relevant steady states. In this paper, we design a well-balanced numerical scheme for the shallow water magnetohydrodynamic system with topography, that resolves exactly a large family of steady states. It is obtained by a generalized hydrostatic reconstruction algorithm involving the magnetic field. It is positive in height and semi-discrete entropy satisfying, which ensures the robustness of the scheme.

Keywords: Shallow water magnetohydrodynamics, topography, well-balanced scheme, hydrostatic reconstruction, semi-discrete entropy inequality.

Mathematics Subject Classification: 76W05, 76M12, 35L65

1 Introduction

The shallow water magnetohydrodynamic (SWMHD) system has been introduced in [20] to describe the thin layer evolution of the solar tachocline. It is written in 2d in the tangent plane approximation as

$$\partial_t h + \nabla \cdot (h\mathbf{u}) = 0, \quad (1.1)$$

$$\partial_t (h\mathbf{u}) + \nabla \cdot (h\mathbf{u} \otimes \mathbf{u} - h\mathbf{b} \otimes \mathbf{b}) + \nabla (gh^2/2) + gh\nabla z + fh\mathbf{u}^\perp = 0, \quad (1.2)$$

$$\partial_t (h\mathbf{b}) + \nabla \cdot (h\mathbf{b} \otimes \mathbf{u} - h\mathbf{u} \otimes \mathbf{b}) + \mathbf{u} \nabla \cdot (h\mathbf{b}) = 0, \quad (1.3)$$

where $g > 0$ is the gravity constant, $h \geq 0$ is the thickness of the fluid, $\mathbf{u} = (u, v)$ is the velocity, $\mathbf{b} = (a, b)$ is the magnetic field, $z(x)$ is the topography, $f(x)$ is the Coriolis parameter, and \mathbf{u}^\perp denotes the vector obtained from \mathbf{u} by a rotation of angle $\pi/2$. The notation $\nabla \cdot (\mathbf{b} \otimes \mathbf{u})$ is for the vector with index i given by $\sum_j \partial_j (b_i u_j)$. The system has to be completed with the entropy (energy) inequality

$$\begin{aligned} & \partial_t \left(\frac{1}{2} h |\mathbf{u}|^2 + \frac{1}{2} g h^2 + \frac{1}{2} h |\mathbf{b}|^2 + g h z \right) \\ & + \nabla \cdot \left(\left(\frac{1}{2} h |\mathbf{u}|^2 + g h^2 + \frac{1}{2} h |\mathbf{b}|^2 + g h z \right) \mathbf{u} - h \mathbf{b} (\mathbf{b} \cdot \mathbf{u}) \right) \leq 0, \end{aligned} \quad (1.4)$$

*Université Paris-Est, Laboratoire d'Analyse et de Mathématiques Appliquées (UMR 8050), CNRS, UPEM, UPEC, F-77454, Marne-la-Vallée, France (François.Bouchut@u-pem.fr), (Xavier.Lhebrard@u-pem.fr)

that becomes an equality in the absence of shocks. We recall that extra term $\mathbf{u}\nabla \cdot (h\mathbf{b})$ in the induction equation (1.3), that has been proposed in [16], is put for 2d numerical purposes only, while the physically relevant situation is $\nabla \cdot (h\mathbf{b}) = 0$.

In the one and a half dimensional setting, i.e. if dependency is only in one spatial variable x , the system simplifies to

$$\partial_t h + \partial_x(hu) = 0, \quad (1.5)$$

$$\partial_t(hu) + \partial_x(hu^2 + P) + gh\partial_x z - fhv = 0, \quad (1.6)$$

$$\partial_t(hv) + \partial_x(huv + P_\perp) + fhu = 0, \quad (1.7)$$

$$\partial_t(ha) + u\partial_x(ha) = 0, \quad (1.8)$$

$$\partial_t(hb) + \partial_x(hbu - hav) + v\partial_x(ha) = 0, \quad (1.9)$$

with

$$P = g\frac{h^2}{2} - ha^2, \quad P_\perp = -hab, \quad (1.10)$$

and the energy inequality (1.4) becomes

$$\begin{aligned} & \partial_t \left(\frac{1}{2}h(u^2 + v^2) + \frac{1}{2}gh^2 + \frac{1}{2}h(a^2 + b^2) + ghz \right) \\ & + \partial_x \left(\left(\frac{1}{2}h(u^2 + v^2) + gh^2 + \frac{1}{2}h(a^2 + b^2) + ghz \right)u - ha(au + bv) \right) \leq 0. \end{aligned} \quad (1.11)$$

According to [17], the eigenvalues of the system (1.5)-(1.9) are $u, u \pm |a|, u \pm \sqrt{a^2 + gh}$. The associated waves are called respectively material (or divergence) waves, Alfvén waves and magnetogravity waves. It is classical in shallow water systems to consider the topography z as an additional variable to the system, satisfying $\partial_t z = 0$. In this setting there is an additional eigenvalue which is 0, and we shall call the associated wave the topography wave. The presence of the zero-order Coriolis terms proportional to f induces indeed more complex nonlinear waves [27]. These are studied numerically in [9]. In the present work, from now on we shall always assume that $f \equiv 0$.

The system (1.5)-(1.9) is nonconservative in the variables ha, hb . However, ha jumps only through the material contacts, where u and v are continuous. Therefore, there is indeed no ambiguity in the non conservative products $u\partial_x(ha)$ and $v\partial_x(ha)$, that are well-defined. Concerning the nonconservative term $h\partial_x z$ in (1.6), it is well-defined for continuous topography z . Piecewise constant discontinuous z is considered however for discrete approximations.

A striking property of the system (1.5)-(1.9) is that four out of six of the waves are contact discontinuities, corresponding to linearly degenerate eigenvalues: the material contacts associated to the eigenvalue u , the left Alfvén contacts associated to $u - |a|$, the right Alfvén contacts associated to $u + |a|$, and the topography contacts associated to the eigenvalue 0. Resonance can occur, which means that these waves can collapse. It happens in particular when $u = 0$ or $u \pm |a| = 0$.

Multidimensional simulations of the SWMHD system have been performed in [23, 24, 25]. As for the compressible MHD system, one-dimensional solvers that are accurate on contact waves are needed in order to reduce significantly the numerical diffusion in complex and multidimensional settings, that generically

involve Alfvén waves, see for example [18, 5]. At the same time, the robustness of the scheme must be maintained.

Well-balanced finite volume schemes for solving shallow water type models with topography have been extensively developed, see [6] and the references therein. A main principle in such schemes is to resolve exactly some steady states, in order to reduce significantly the numerical viscosity. The same question arises for hydrodynamic systems without topography, when linearly degenerate eigenvalues are involved. Indeed, in the numerical simulation of conservation laws, shocks are generally better resolved than contact discontinuities because of their compressive nature. This is why it is important to resolve well the contact discontinuities, that do not benefit of any compressive effect. In the SWMHD system (1.5)-(1.9), we have at the same time “dynamic” linearly degenerate eigenvalues (material and Alfvén contact waves), and the “static” linearly degenerate eigenvalue (steady topography contact waves). The aim of this paper is to build a well-balanced scheme for the SWMHD system (1.5)-(1.9) that is accurate on all these contact waves. It follows [8], where we built an entropy satisfying approximate Riemann solver for the SWMHD system without topography that is accurate on all contact waves.

A generic tool for building well-balanced schemes that we use is the hydrostatic reconstruction method, that has been introduced in [1]. One of its strengths is that it enforces a semi-discrete entropy inequality, ensuring the robustness of the scheme and the computation of entropic shocks. Several variants and extensions have been proposed in [6, 13, 10, 11, 7]. Other approaches are the Roe method [2, 22, 21, 14, 12], the approximate Riemann solver method [19, 4, 3]. Central schemes are used also, and can handle multi steady states [15]. Higher-order extensions are reviewed in [26].

The paper is organized as follows. In Section 2 we describe the steady states of the SWMHD system with topography. In Section 3 we write down our numerical scheme, and in particular the reconstruction involved in the numerical fluxes, and our main result Theorem 3.1. Section 4 is devoted to the proof of this theorem. Finally, in Section 5 we perform numerical tests.

2 Steady states

As mentioned above, the system with topography (1.5)-(1.9) with $f \equiv 0$ has four linearly degenerate eigenvalues $u - |a|$, u , $u + |a|$ and 0, that can be resonant. We would like to build a scheme that is well-balanced for some contact waves for the eigenvalue 0, that are in particular steady states. Several cases can be considered. For each of them, it is straightforward to check that the following relations define steady states.

- Non-resonant case ($u \neq 0$ and $u \pm a \neq 0$). The relations are

$$\begin{aligned} hu = cst (\neq 0), \quad ha = cst (\neq \pm hu), \quad v = cst, \quad b = cst, \\ \frac{u^2}{2} - \frac{a^2}{2} + g(h+z) = cst. \end{aligned} \tag{2.1}$$

As in the classical shallow water system, we shall not consider these steady states for the well-balanced property, because they are too complicated to handle (see however [10]).

- Material resonant case ($u = 0$ and $a \neq 0$). The differential relations are

$$\begin{aligned} u &= 0, \quad v = cst, \quad hab = cst, \\ \partial_x \left(g \frac{h^2}{2} - ha^2 \right) + gh \partial_x z &= 0. \end{aligned} \quad (2.2)$$

Note that in contrast with the other cases, the second line in (2.2) is not integrable. It implies that for discontinuous data, this differential relation can have different possible interpretations in terms of nonconservative products.

We shall consider indeed a particular subfamily of steady states from (2.2), characterized by the relation $\sqrt{h} a = cst$, which yields

$$u = 0, \quad v = cst, \quad h + z = cst, \quad \sqrt{h} a = cst (\neq 0), \quad \sqrt{h} b = cst. \quad (2.3)$$

- Alfvén resonant case ($u \neq 0$ and $u \pm a = 0$). The relations are

$$hu = cst (\neq 0), \quad ha = \mp hu, \quad h + z = cst, \quad v \pm b = cst. \quad (2.4)$$

- Material and Alfvén resonant case ($u = a = 0$). The relations are

$$u = 0, \quad a = 0, \quad h + z = cst. \quad (2.5)$$

3 Formulas for the numerical fluxes, and main result

A finite volume scheme for the nonconservative system (1.5)-(1.9) with $f \equiv 0$ can be written

$$U_i^{n+1} = U_i^n - \frac{\Delta t}{\Delta x_i} \left(F_l(U_i^n, U_{i+1}^n, \Delta z_{i+1/2}) - F_r(U_{i-1}^n, U_i^n, \Delta z_{i-1/2}) \right), \quad (3.1)$$

where

$$U = (h, hu, hv, ha, hb), \quad (3.2)$$

and as usual n stands for the time index, i for the space location, and $\Delta z_{i+1/2} = z_{i+1} - z_i$. Thus we need to define the left and right numerical fluxes $F_l(U_l, U_r, \Delta z)$, $F_r(U_l, U_r, \Delta z)$, for all left and right values U_l, U_r, z_l, z_r with $\Delta z = z_r - z_l$.

We use the hydrostatic reconstruction method of [1]. Denoting the left and right states by $U_l = (h_l, h_l u_l, h_l v_l, h_l a_l, h_l b_l)$, $U_r = (h_r, h_r u_r, h_r v_r, h_r a_r, h_r b_r)$, we define the reconstructed heights

$$h_l^\# = (h_l - (\Delta z)_+)_+, \quad h_r^\# = (h_r - (-\Delta z)_+)_+, \quad (3.3)$$

with the notation $x_+ \equiv \max(0, x)$. We also define new reconstructed magnetic states

$$a_l^\# = \kappa_l a_l, \quad a_r^\# = \kappa_r a_r, \quad (3.4)$$

$$b_l^\# = \kappa_l b_l, \quad b_r^\# = \kappa_r b_r, \quad (3.5)$$

with

$$\kappa_l = \min \left(\sqrt{\frac{h_l}{h_l^\#}}, \gamma \right), \quad \kappa_r = \min \left(\sqrt{\frac{h_r}{h_r^\#}}, \gamma \right), \quad (3.6)$$

and where $\gamma \geq 1$ is a cutoff parameter. We define finally the left and right reconstructed states as

$$U_l^\# = \left(h_l^\#, h_l^\# u_l, h_l^\# v_l, h_l^\# a_l^\#, h_l^\# b_l^\# \right), \quad U_r^\# = \left(h_r^\#, h_r^\# u_r, h_r^\# v_r, h_r^\# a_r^\#, h_r^\# b_r^\# \right). \quad (3.7)$$

Note that we use the notation $\#$ instead of $*$ in order to avoid confusions with intermediate states of Riemann solvers. Then the numerical fluxes are defined by

$$\begin{aligned} F_l(U_l, U_r, \Delta z) &= \mathcal{F}_l(U_l^\#, U_r^\#) \\ &+ \left(0, g \frac{h_l^2}{2} - g \frac{h_l^{\#2}}{2}, 0, (\kappa_l(ha)_l^\# - (ha)_l) u_l, (\kappa_l(ha)_l^\# - (ha)_l) v_l \right) \\ &+ (\kappa_l - 1) \left(0, 0, 0, \mathcal{F}_l^{ha}(U_l^\#, U_r^\#), \mathcal{F}_l^{hb}(U_l^\#, U_r^\#) \right) \\ &+ \mathcal{F}^h(U_l^\#, U_r^\#) \left(0, 0, 0, \frac{a_l}{2}(1 - \kappa_l^2), \frac{b_l}{2}(1 - \kappa_l^2) \right), \\ F_r(U_l, U_r, \Delta z) &= \mathcal{F}_r(U_l^\#, U_r^\#) \\ &+ \left(0, g \frac{h_r^2}{2} - g \frac{h_r^{\#2}}{2}, 0, (\kappa_r(ha)_r^\# - (ha)_r) u_r, (\kappa_r(ha)_r^\# - (ha)_r) v_r \right) \\ &+ (\kappa_r - 1) \left(0, 0, 0, \mathcal{F}_r^{ha}(U_l^\#, U_r^\#), \mathcal{F}_r^{hb}(U_l^\#, U_r^\#) \right) \\ &+ \mathcal{F}^h(U_l^\#, U_r^\#) \left(0, 0, 0, \frac{a_r}{2}(1 - \kappa_r^2), \frac{b_r}{2}(1 - \kappa_r^2) \right), \end{aligned} \quad (3.8)$$

where \mathcal{F}_l and \mathcal{F}_r are the numerical fluxes of [8] associated to the problem without topography, and \mathcal{F}^h is its common left/right height flux.

Theorem 3.1. *The scheme (3.1) with the numerical fluxes F_l , F_r defined by (3.8) satisfies the following properties.*

- (i) *It is conservative in the variables h and hv ,*
- (ii) *It is consistent with (1.5)-(1.9) for smooth solutions,*
- (iii) *It keeps the positivity of h under the CFL condition $\Delta t A(U_l^\#, U_r^\#) \leq \frac{1}{2} \min(\Delta x_l, \Delta x_r)$ with $A(.,.)$ the maximum speed of the homogeneous solver, defined by [8, eq. (4.8)],*
- (iv) *It satisfies a semi-discrete energy inequality associated to (1.11),*
- (v) *It is well-balanced with respect to steady material and Alfvén contact discontinuities without jump in topography,*
- (vi) *Under the condition*

$$\gamma \geq \max \left(\sqrt{\frac{h_l}{h_l^\#}}, \sqrt{\frac{h_r}{h_r^\#}} \right) \quad (3.9)$$

on the parameter γ appearing in (3.6), it is well-balanced with respect to the steady states (2.3) corresponding to material resonance,

(vii) *It is well-balanced with respect to the steady states (2.5) corresponding to material and Alfvén resonance.*

The proof of Theorem 3.1 is given in Section 4, and we give here some comments on this result.

- The formulas (3.8) for the numerical fluxes are defined exactly so that the proof of the entropy inequality is an identity. Then it follows that the scheme is consistent.
- The cutoff parameter γ is put in order to prevent κ_l, κ_r to be too large. Without it one would have possibly large $a_l^\#, a_r^\#$ and as a consequence a very restrictive CFL condition stated in (iii).
- The particular values (3.6) of κ_l, κ_r are involved only in the well-balanced property (vi), and do not matter for the other properties. We only need that their value is 1 when $\Delta z = 0$. In particular, if $\gamma = 1$, we get $\kappa_l = \kappa_r = 1$ (but then we lose the property (vi)). One can use also different formulas like

$$\kappa_l = \min\left(\frac{h_l}{h_l^\#}, \gamma\right), \quad \kappa_r = \min\left(\frac{h_r}{h_r^\#}, \gamma\right), \quad (3.10)$$

the idea being to have, if γ is large enough, $\kappa_l = h_l/h_l^\#, \kappa_r = h_r/h_r^\#, h_l^\# a_l^\# = h_l a_l, h_r^\# a_r^\# = h_r a_r$. However, with (3.10) or with (3.6), the scheme does not leave invariant the data satisfying $ha = cst$, unfortunately.

- Instead of (2.3), one can consider another subfamily of steady states from (2.2), characterized by the relation $ha = cst$. It leads to consider the steady states

$$u = 0, \quad v = cst, \quad ha = cst (\neq 0), \quad b = cst, \quad h - \frac{a^2}{2g} + z = cst, \quad (3.11)$$

which are indeed the limit of (2.1) when $hu \rightarrow 0$. An interesting question would be to design a scheme that is well-balanced with respect to this family instead of (2.3).

4 Proof of Theorem 3.1

The proof of (i), i.e. $F_l^h = F_r^h, F_l^{hv} = F_r^{hv}$, is obvious from formulas (3.8) since the homogeneous solver already satisfies this property. We omit the proof of (iii), which follows the proof of Proposition 4.14 in [6].

The property (v) is inherited from the homogeneous solver that is described in [8], since

$$\Delta z = 0 \quad \text{implies} \quad F_l(U_l, U_r, 0) = \mathcal{F}_l(U_l, U_r), \quad F_r(U_l, U_r, 0) = \mathcal{F}_r(U_l, U_r). \quad (4.1)$$

We recall more explicitly that, defining

$$F(U) = (hu, hu^2 + P, huv + P_\perp, 0, hbu - hav), \quad (4.2)$$

this property of well-balancing for the homogeneous solver means that $\mathcal{F}_l(U_l, U_r) = F(U_l)$ and $\mathcal{F}_r(U_l, U_r) = F(U_r)$ for all data of the form:

$$u_l = u_r = 0, v_l = v_r, P(U_l) = P(U_r), P_\perp(U_l) = P_\perp(U_r), \quad (4.3)$$

or

$$h_l = h_r, a_l = a_r \neq 0, u_l = u_r = |a_l|, b_l \operatorname{sgn}(a_l) - v_l = b_r \operatorname{sgn}(a_r) - v_r, \quad (4.4)$$

or

$$h_l = h_r, a_l = a_r \neq 0, u_l = u_r = -|a_l|, b_l \operatorname{sgn}(a_l) + v_l = b_r \operatorname{sgn}(a_r) + v_r, \quad (4.5)$$

or

$$h_l = h_r, u_l = u_r = 0, a_l = a_r = 0. \quad (4.6)$$

For the proof of (vi), consider data U_l, U_r, z_l, z_r satisfying (2.3), i.e. $u_l = u_r = 0$, $v_l = v_r$, $h_l + z_l = h_r + z_r$, $\sqrt{h_l}a_l = \sqrt{h_r}a_r$, $\sqrt{h_l}b_l = \sqrt{h_r}b_r$. Then from (3.3) we get

$$h_l^\# = h_r^\# \equiv h^\#, \quad (4.7)$$

the common value $h^\#$ being h_r if $\Delta z \geq 0$, or h_l if $\Delta z \leq 0$. Using condition (3.9), according to (3.4), (3.5), (3.6), we get $\kappa_l = \sqrt{h_l/h_l^\#}$, $\kappa_r = \sqrt{h_r/h_r^\#}$, $\sqrt{h_l^\#}a_l^\# = \sqrt{h_l}a_l$, $\sqrt{h_r^\#}a_r^\# = \sqrt{h_r}a_r$, $\sqrt{h_l^\#}b_l^\# = \sqrt{h_l}b_l$, $\sqrt{h_r^\#}b_r^\# = \sqrt{h_r}b_r$. Thus

$$\sqrt{h_l^\#}a_l^\# = \sqrt{h_r^\#}a_r^\#, \quad \sqrt{h_l^\#}b_l^\# = \sqrt{h_r^\#}b_r^\#. \quad (4.8)$$

Using (4.7), (4.8), we get

$$U_l^\# = U_r^\# \equiv U^\# \equiv (h^\#, 0, h^\#v^\#, h^\#a^\#, h^\#b^\#). \quad (4.9)$$

We observe that then $\mathcal{F}_l(U_l^\#, U_r^\#) = \mathcal{F}_r(U_l^\#, U_r^\#) = F(U^\#)$, and that indeed

$$F(U^\#) = (0, g(h^\#)^2/2 - h^\#(a^\#)^2, -h^\#a^\#b^\#, 0, -h^\#a^\#v^\#). \quad (4.10)$$

The formulas (3.8) yield

$$F_l = \left(0, g(h_l)^2/2 - h_l(a_l)^2, -h_l a_l b_l, 0, -h_l a_l v_l\right) = F(U_l), \quad (4.11)$$

$$F_r = \left(0, g(h_r)^2/2 - h_r(a_r)^2, -h_r a_r b_r, 0, -h_r a_r v_r\right) = F(U_r), \quad (4.12)$$

which proves the claim.

For the proof of (vii), consider data U_l, U_r, z_l, z_r satisfying (2.5), i.e. $u_l = u_r = 0$, $h_l + z_l = h_r + z_r$, $a_l = a_r = 0$. Then we get $h_l^\# = h_r^\#$, $u_l^\# = u_r^\# = 0$, $a_l^\# = a_r^\# = 0$, and the fluxes $\mathcal{F}_l, \mathcal{F}_r$ are evaluated on states $U_l^\#, U_r^\#$ of the type (4.6). Thus $\mathcal{F}_l(U_l^\#, U_r^\#) = F(U_l^\#)$ and $\mathcal{F}_r(U_l^\#, U_r^\#) = F(U_r^\#)$. Plugging this in (3.8), we obtain $F_l = F(U_l)$, $F_r = F(U_r)$, which proves the claim.

4.1 Consistency

In order to get (ii) in Theorem 3.1 in the sense of Definition 4.2 in [6], we need to prove that

$$F_l(U, U, 0) = F_r(U, U, 0) = F(U), \quad (4.13)$$

and that as $U_l \rightarrow U$, $U_r \rightarrow U$, $\Delta z \rightarrow 0$,

$$\begin{aligned} F_r(U_l, U_r, \Delta z) - F_l(U_l, U_r, \Delta z) &= -B(u, v)((ha)_r - (ha)_l) \\ &+ \left(0, -gh\Delta z, 0, 0, 0\right) + o(|U_l - U| + |U_r - U| + |\Delta z|), \end{aligned} \quad (4.14)$$

with

$$B(u, v) = (0, 0, 0, u, v). \quad (4.15)$$

The consistency with the exact flux (4.13) is obviously satisfied because of the property (4.1). In order to prove the consistency with the source (4.14), we write

$$\begin{aligned} &F_r(U_l, U_r, \Delta z) - F_l(U_l, U_r, \Delta z) \\ &= \mathcal{F}_r(U_l^\#, U_r^\#) - \mathcal{F}_l(U_l^\#, U_r^\#) \\ &+ B(u_r, v_r) \left(\kappa_r (ha)_r^\# - (ha)_r \right) - B(u_l, v_l) \left(\kappa_l (ha)_l^\# - (ha)_l \right) \\ &+ (\kappa_r - 1) \left(0, 0, 0, \mathcal{F}_r^{ha}(U_l^\#, U_r^\#), \mathcal{F}_r^{hb}(U_l^\#, U_r^\#) \right) \\ &- (\kappa_l - 1) \left(0, 0, 0, \mathcal{F}_l^{ha}(U_l^\#, U_r^\#), \mathcal{F}_l^{hb}(U_l^\#, U_r^\#) \right) \\ &+ \mathcal{F}^h(U_l^\#, U_r^\#) \left(0, 0, 0, \frac{a_r}{2}(1 - \kappa_r^2), \frac{b_r}{2}(1 - \kappa_r^2) \right) \\ &- \mathcal{F}^h(U_l^\#, U_r^\#) \left(0, 0, 0, \frac{a_l}{2}(1 - \kappa_l^2), \frac{b_l}{2}(1 - \kappa_l^2) \right) \\ &+ \left(0, g \frac{h_l^{\#2}}{2} - g \frac{h_l^2}{2} + g \frac{h_r^2}{2} - g \frac{h_r^{\#2}}{2}, 0, 0, 0 \right). \end{aligned} \quad (4.16)$$

Let us denote $\Delta = |U_l - U| + |U_r - U| + |\Delta z|$. When $U_l, U_r \rightarrow U$ and $\Delta z \rightarrow 0$ one has from (3.3)-(3.7) $\kappa_l - 1 = O(\Delta)$, $\kappa_r - 1 = O(\Delta)$, and thus $U_l^\# - U = O(\Delta)$, $U_r^\# - U = O(\Delta)$ (we consider only the case $h > 0$ here). Then the consistency of the numerical flux without source obtained in [8] gives

$$\mathcal{F}_r(U_l^\#, U_r^\#) - \mathcal{F}_l(U_l^\#, U_r^\#) = -B(u, v) \left((ha)_r^\# - (ha)_l^\# \right) + o(\Delta). \quad (4.17)$$

Next, we have

$$B(u_r, v_r) \left(\kappa_r (ha)_r^\# - (ha)_r \right) = B(u, v) \left(\kappa_r (ha)_r^\# - (ha)_r \right) + o(\Delta), \quad (4.18)$$

and

$$B(u_l, v_l) \left(\kappa_l (ha)_l^\# - (ha)_l \right) = B(u, v) \left(\kappa_l (ha)_l^\# - (ha)_l \right) + o(\Delta). \quad (4.19)$$

Summing up (4.17), (4.18), (4.19), we obtain

$$\begin{aligned}
& \mathfrak{F}_r(U_l^\#, U_r^\#) - \mathfrak{F}_l(U_l^\#, U_r^\#) \\
& + B(u_r, v_r) \left(\kappa_r (ha)_r^\# - (ha)_r \right) - B(u_l, v_l) \left(\kappa_l (ha)_l^\# - (ha)_l \right) \\
= & B(u, v) (\kappa_r - 1) (ha)_r^\# - B(u, v) (\kappa_l - 1) (ha)_l^\# \\
& - B(u, v) \left((ha)_r - (ha)_l \right) + o(\Delta). \\
= & B(u, v) (\kappa_r - 1) (ha) - B(u, v) (\kappa_l - 1) (ha) \\
& - B(u, v) \left((ha)_r - (ha)_l \right) + o(\Delta).
\end{aligned} \tag{4.20}$$

Now we look at the terms in the right-hand side of (4.16) from the third to the sixth line. Using that $\mathfrak{F}_l^{ha}(U, U) = \mathfrak{F}_r^{ha}(U, U) = 0$ and $\mathfrak{F}_l^{hb}(U, U) = \mathfrak{F}_r^{hb}(U, U) = hbu - hav$, we deduce

$$\begin{aligned}
& (\kappa_r - 1) \left(0, 0, 0, \mathfrak{F}_r^{ha}(U_l^\#, U_r^\#), \mathfrak{F}_r^{hb}(U_l^\#, U_r^\#) \right) \\
= & (\kappa_r - 1) \left(0, 0, 0, 0, hbu - hav \right) + o(\Delta),
\end{aligned} \tag{4.21}$$

and

$$\begin{aligned}
& -(\kappa_l - 1) \left(0, 0, 0, \mathfrak{F}_l^{ha}(U_l^\#, U_r^\#), \mathfrak{F}_l^{hb}(U_l^\#, U_r^\#) \right) \\
= & -(\kappa_l - 1) \left(0, 0, 0, 0, hbu - hav \right) + o(\Delta).
\end{aligned} \tag{4.22}$$

Writing $1 - \kappa_r^2 = (1 + \kappa_r)(1 - \kappa_r)$, we get asymptotically

$$\frac{a_r}{2} (1 - \kappa_r^2) = a(1 - \kappa_r) + o(\Delta). \tag{4.23}$$

Similarly, we have

$$\frac{a_l}{2} (1 - \kappa_l^2) = a(1 - \kappa_l) + o(\Delta), \tag{4.24}$$

$$\frac{b_r}{2} (1 - \kappa_r^2) = b(1 - \kappa_r) + o(\Delta), \tag{4.25}$$

$$\frac{b_l}{2} (1 - \kappa_l^2) = b(1 - \kappa_l) + o(\Delta). \tag{4.26}$$

Using (4.23), (4.24), (4.25), (4.26) and the property $\mathfrak{F}^h(U, U) = hu$, we obtain

$$\begin{aligned}
& \mathfrak{F}^h(U_l^\#, U_r^\#) \left(0, 0, 0, \frac{a_r}{2} (1 - \kappa_r^2), \frac{b_r}{2} (1 - \kappa_r^2) \right) \\
= & \left(0, 0, 0, hua(1 - \kappa_r), hub(1 - \kappa_r) \right) + o(\Delta),
\end{aligned} \tag{4.27}$$

$$\begin{aligned}
& -\mathfrak{F}^h(U_l^\#, U_r^\#) \left(0, 0, 0, \frac{a_l}{2} (1 - \kappa_l^2), \frac{b_l}{2} (1 - \kappa_l^2) \right) \\
= & -\left(0, 0, 0, hua(1 - \kappa_l), hub(1 - \kappa_l) \right) + o(\Delta).
\end{aligned} \tag{4.28}$$

The sum of (4.21), (4.22), (4.27), (4.28) gives the asymptotic formula

$$\begin{aligned}
& (\kappa_r - 1) \left(0, 0, 0, \mathfrak{F}_r^{ha}(U_l^\#, U_r^\#), \mathfrak{F}_r^{hb}(U_l^\#, U_r^\#) \right) \\
& -(\kappa_l - 1) \left(0, 0, 0, \mathfrak{F}_l^{ha}(U_l^\#, U_r^\#), \mathfrak{F}_l^{hb}(U_l^\#, U_r^\#) \right) \\
& + \mathfrak{F}^h(U_l^\#, U_r^\#) \left(0, 0, 0, \frac{a_r}{2} (1 - \kappa_r^2), \frac{b_r}{2} (1 - \kappa_r^2) \right) \\
& - \mathfrak{F}^h(U_l^\#, U_r^\#) \left(0, 0, 0, \frac{a_l}{2} (1 - \kappa_l^2), \frac{b_l}{2} (1 - \kappa_l^2) \right) \\
= & -B(u, v) (\kappa_r - 1) (ha) + B(u, v) (\kappa_l - 1) (ha) + o(\Delta).
\end{aligned} \tag{4.29}$$

Adding (4.20) and (4.29), we obtain the consistency of the nonconservative magnetic terms

$$\begin{aligned}
& \mathcal{F}_r(U_l^\#, U_r^\#) - \mathcal{F}_l(U_l^\#, U_r^\#) \\
& + B(u_r, v_r) \left(\kappa_r (ha)_r^\# - (ha)_r \right) - B(u_l, v_l) \left(\kappa_l (ha)_l^\# - (ha)_l \right) \\
& + (\kappa_r - 1) \left(0, 0, 0, \mathcal{F}_r^{ha}(U_l^\#, U_r^\#), \mathcal{F}_r^{hb}(U_l^\#, U_r^\#) \right) \\
& - (\kappa_l - 1) \left(0, 0, 0, \mathcal{F}_l^{ha}(U_l^\#, U_r^\#), \mathcal{F}_l^{hb}(U_l^\#, U_r^\#) \right) \\
& + \mathcal{F}^h(U_l^\#, U_r^\#) \left(0, 0, 0, \frac{a_r}{2}(1 - \kappa_r^2), \frac{b_r}{2}(1 - \kappa_r^2) \right) \\
& - \mathcal{F}^h(U_l^\#, U_r^\#) \left(0, 0, 0, \frac{a_l}{2}(1 - \kappa_l^2), \frac{b_l}{2}(1 - \kappa_l^2) \right) \\
& = -B(u, v) \left((ha)_r - (ha)_l \right) + o(\Delta).
\end{aligned} \tag{4.30}$$

Finally, as in the unmodified hydrostatic reconstruction scheme, the last line in (4.16) gives the nonconservative topography term

$$\left(0, g \frac{h_l^{\#2}}{2} - g \frac{h_l^2}{2} + g \frac{h_r^2}{2} - g \frac{h_r^{\#2}}{2}, 0, 0, 0 \right) = (0, -gh\Delta z, 0, 0, 0) + o(\Delta). \tag{4.31}$$

With (4.30), all the terms in (4.16) have been expanded, and we get (4.14).

4.2 Entropy inequality

Let us finally prove the property (iv) in Theorem 3.1. At the continuous level, the energy inequality (1.11) can be written

$$\partial_t \tilde{E} + \partial_x \tilde{G} \leq 0, \tag{4.32}$$

with

$$\tilde{E}(U, z) = E(U) + ghz, \quad \tilde{G}(U, z) = G(U) + ghzu, \tag{4.33}$$

and

$$\begin{aligned}
E(U) &= \frac{1}{2}h(u^2 + v^2) + \frac{1}{2}gh^2 + \frac{1}{2}h(a^2 + b^2), \\
G(U) &= E(U)u + P(U)u + \tilde{P}_\perp(U)v.
\end{aligned} \tag{4.34}$$

As before, $U = (h, hu, hv, ha, hb)$ and P, P_\perp are defined by (1.10). As proved in [8], the scheme without topography satisfies a fully discrete energy inequality. According to [6, section 2.2.2], it implies that it satisfies also a semi-discrete energy inequality, under the form

$$\begin{aligned}
G(U_r) + E'(U_r) (\mathcal{F}_r(U_l, U_r) - F(U_r)) &\leq \mathcal{G}(U_l, U_r), \\
\mathcal{G}(U_l, U_r) &\leq G(U_l) + E'(U_l) (\mathcal{F}_l(U_l, U_r) - F(U_l)),
\end{aligned} \tag{4.35}$$

for all values of U_l, U_r , where E' is the derivative of E with respect to U , F is defined in (4.2), and $\mathcal{G}(U_l, U_r)$ is a consistent energy flux.

Then, for the scheme with topography, the characterization of the semi-discrete energy inequality writes

$$\begin{aligned}
\tilde{G}(U_r, z_r) + \tilde{E}'(U_r, z_r) (F_r - F(U_r)) &\leq \tilde{\mathcal{G}}(U_l, U_r, z_l, z_r), \\
\tilde{\mathcal{G}}(U_l, U_r, z_l, z_r) &\leq \tilde{G}(U_l, z_l) + \tilde{E}'(U_l, z_l) (F_l - F(U_l)),
\end{aligned} \tag{4.36}$$

where \tilde{E} and \tilde{G} are defined by (4.33), \tilde{E}' is the derivative of \tilde{E} with respect to U , and $\tilde{\mathcal{G}}$ is an unknown consistent numerical energy flux. Let us choose

$$\tilde{\mathcal{G}}(U_l, U_r, z_l, z_r) = \mathcal{G}(U_l^\#, U_r^\#) + \mathcal{F}^h(U_l^\#, U_r^\#)gz^\#, \quad (4.37)$$

where \mathcal{F}^h is the common h-component of \mathcal{F}_l and \mathcal{F}_r , and for some $z^\#$ that is defined below. Then, noticing that $\tilde{E}'(U, z) = E'(U) + gz(1, 0, 0, 0)$, we can write the desired inequalities (4.36) as

$$\begin{aligned} & G(U_r) + E'(U_r)(F_r - F(U_r)) + \mathcal{F}^h(U_l^\#, U_r^\#)gz_r \\ & \leq \mathcal{G}(U_l^\#, U_r^\#) + \mathcal{F}^h(U_l^\#, U_r^\#)gz^\#, \end{aligned} \quad (4.38)$$

$$\begin{aligned} & \mathcal{G}(U_l^\#, U_r^\#) + \mathcal{F}^h(U_l^\#, U_r^\#)gz^\# \\ & \leq G(U_l) + E'(U_l)(F_l - F(U_l)) + \mathcal{F}^h(U_l^\#, U_r^\#)gz_l. \end{aligned} \quad (4.39)$$

By using (4.35) evaluated at $U_l^\#, U_r^\#$ and comparing the result with (4.38) and (4.39), we get the sufficient conditions

$$\begin{aligned} & G(U_r) + E'(U_r)(F_r - F(U_r)) + \mathcal{F}^h(U_l^\#, U_r^\#)gz_r \\ & \leq G(U_r^\#) + E'(U_r^\#)(\mathcal{F}_r(U_l^\#, U_r^\#) - F(U_r^\#)) + \mathcal{F}^h(U_l^\#, U_r^\#)gz^\#, \end{aligned} \quad (4.40)$$

$$\begin{aligned} & G(U_l^\#) + E'(U_l^\#)(\mathcal{F}_l(U_l^\#, U_r^\#) - F(U_l^\#)) + \mathcal{F}^h(U_l^\#, U_r^\#)gz^\# \\ & \leq G(U_l) + E'(U_l)(F_l - F(U_l)) + \mathcal{F}^h(U_l^\#, U_r^\#)gz_l. \end{aligned} \quad (4.41)$$

Let us focus on (4.40), that can be rewritten as

$$\begin{aligned} & \left[G - E'F \right]_{r^\#}^r + E'(U_r)F_r - E'(U_r^\#)\mathcal{F}_r(U_l^\#, U_r^\#) \\ & \quad + g(z_r - z^\#)\mathcal{F}^h(U_l^\#, U_r^\#) \leq 0, \end{aligned} \quad (4.42)$$

with

$$\left[G - E'F \right]_{r^\#}^r \equiv \left(G(U_r) - E'(U_r)F(U_r) \right) - \left(G(U_r^\#) - E'(U_r^\#)F(U_r^\#) \right). \quad (4.43)$$

We compute now

$$E'(U) = \left(-(u^2 + v^2)/2 + gh - (a^2 + b^2)/2, u, v, a, b \right), \quad (4.44)$$

and using (4.34), (4.2), we deduce the identity

$$G(U) - E'(U)F(U) = -g\frac{h^2}{2}u + ha(au + bv) = -P(U)u - P_\perp(U)v. \quad (4.45)$$

Then, according to the definition (3.8) of F_r ,

$$\begin{aligned} E'(U_r)F_r &= E'(U_r)\mathcal{F}_r(U_l^\#, U_r^\#) \\ &+ E'(U_r) \left(0, g\frac{h_r^2}{2} - g\frac{h_r^{\#2}}{2}, 0, \right. \\ & \quad \left. (\kappa_r(ha)_r^\# - (ha)_r)u_r, (\kappa_r(ha)_r^\# - (ha)_r)v_r \right) + Q_r, \end{aligned} \quad (4.46)$$

with

$$Q_r = E'(U_r)(\kappa_r - 1) \left(0, 0, 0, \mathcal{F}_r^{ha}(U_l^\#, U_r^\#), \mathcal{F}_r^{hb}(U_l^\#, U_r^\#) \right) \\ + E'(U_r) \mathcal{F}^h(U_l^\#, U_r^\#) \left(0, 0, 0, \frac{a_r}{2}(1 - \kappa_r^2), \frac{b_r}{2}(1 - \kappa_r^2) \right). \quad (4.47)$$

Using (4.44) and (4.45), we can rewrite (4.46) as

$$E'(U_r)F_r = E'(U_r)\mathcal{F}_r(U_l^\#, U_r^\#) - \left[G - E'F \right]_{r^\#}^r + Q_r. \quad (4.48)$$

Thus the required inequality (4.42) simplifies to

$$\left(E'(U_r) - E'(U_r^\#) \right) \mathcal{F}_r(U_l^\#, U_r^\#) + Q_r + g(z_r - z^\#) \mathcal{F}^h(U_l^\#, U_r^\#) \leq 0. \quad (4.49)$$

Now, on the one side, one can compute

$$Q_r = (\kappa_r - 1)a_r \mathcal{F}_r^{ha}(U_l^\#, U_r^\#) + (\kappa_r - 1)b_r \mathcal{F}_r^{hb}(U_l^\#, U_r^\#) \\ + (1 - \kappa_r^2) \mathcal{F}^h(U_l^\#, U_r^\#) \frac{a_r^2 + b_r^2}{2}. \quad (4.50)$$

On the other side, according to (4.44), we have

$$E'(U_r) - E'(U_r^\#) \\ = \left(g(h_r - h_r^\#) - \frac{a_r^2 + b_r^2}{2} + \frac{(a_r^\#)^2 + (b_r^\#)^2}{2}, 0, 0, a_r - a_r^\#, b_r - b_r^\# \right) \\ = \left(g(h_r - h_r^\#) - (1 - \kappa_r^2) \frac{a_r^2 + b_r^2}{2}, 0, 0, (1 - \kappa_r)a_r, (1 - \kappa_r)b_r \right). \quad (4.51)$$

Using both (4.50) and (4.51), we get

$$\left(E'(U_r) - E'(U_r^\#) \right) \mathcal{F}_r(U_l^\#, U_r^\#) + Q_r = g(h_r - h_r^\#) \mathcal{F}^h(U_l^\#, U_r^\#). \quad (4.52)$$

Plugging this in (4.49), we obtain the sufficient right inequality

$$g(h_r - h_r^\# + z_r - z^\#) \mathcal{F}^h(U_l^\#, U_r^\#) \leq 0. \quad (4.53)$$

A symmetric analysis for the left inequality (4.41) gives similarly

$$g(h_l - h_l^\# + z_l - z^\#) \mathcal{F}^h(U_l^\#, U_r^\#) \geq 0. \quad (4.54)$$

We choose $z^\# = \max(z_l, z_r)$, so that (4.53), (4.54) can be finally put under the form

$$g(h_r - h_r^\# - (-\Delta z)_+) \mathcal{F}^h(U_l^\#, U_r^\#) \leq 0, \\ g(h_l - h_l^\# - (\Delta z)_+) \mathcal{F}^h(U_l^\#, U_r^\#) \geq 0. \quad (4.55)$$

Taking into account (3.3), we observe that if $h_l - (\Delta z)_+ \geq 0$ then the second line of (4.55) is trivial. Otherwise $h_l^\# = 0$ and the second inequality of (4.55) holds because $\mathcal{F}^h(0, U_r^\#) \leq 0$ by the h -nonnegativity of the numerical flux. The same argument is valid for the first inequality of (4.55), which concludes the proof of Theorem 3.1.

5 Numerical tests

In this section we perform numerical computations in order to evaluate the properties of the scheme, in relation with Theorem 3.1. First and second order methods in time and space are evaluated, the latter using an ENO reconstruction, as described in [6, section 4.13]. The conservative variable is U as in (3.2), and the slope limitations are performed on the variables h , $h + z$, u , v , ha , b . We also compare different values of the parameter γ , which is a key to obtain the well-balanced property for steady states of material resonance. We take 200 points, and plot a reference solution obtained by a second order computation with 3300 points. The CFL-number is taken 1/2 in all tests.

Test case - The space variable x is taken in $[0,1]$, $g = 9.81$. Neumann boundary conditions are applied. The test consists of two steady states:

- On $[0,1/2)$, we take initial data corresponding to a steady state in the case of material resonance.
- On $(1/2,1]$, we take initial data corresponding to a steady state in the case of material and Alfvén resonance.

The initial data is sketched on Figure 1 and the numerical values are given in Tables 2 and 3. The solution consists of, from left to right, a material contact, a left rarefaction wave, a left Alfvén contact, a resonant material - right Alfvén contact, and a right shock. We observe that the second order resolution improves the sharpness of contact discontinuities. On Figure 12, we observe that the solution computed with $\gamma = 1$ loses the well-balanced property for the resonant material contact, whereas with $\gamma = 2$ it is well-balanced, which is coherent with point (vi) of Theorem 3.1.

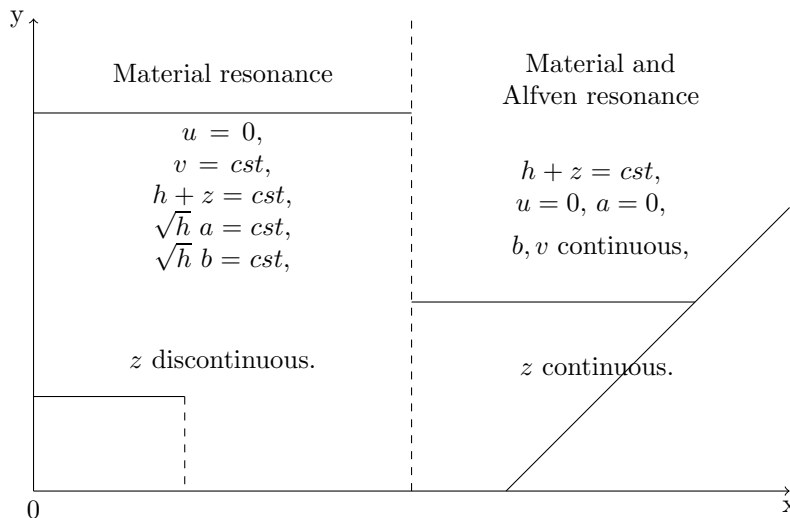


Figure 1: Initial data configuration

Values of x	z	h	u	v	a	b
$x \leq 0.2$	0.5	1.5	0.0	2.0	$1/\sqrt{1.5}$	$2/\sqrt{1.5}$
$0.2 < x \leq 0.5$	0.0	2.0	0.0	2.0	$1/\sqrt{2}$	$2/\sqrt{2}$

Figure 2: Initial data for Material resonance

Values of x	z	h	u	v	a	b
$0.5 < x \leq 0.625$	0.0	0.5	0.0	0.5	0.0	1.0
$0.625 < x \leq 1$	$d(x)$	$(0.5 - d(x))_+$	0.0	$0.5 + d(x)$	0.0	$1.0 + d(x)$

Figure 3: Initial data for Material and Alfven resonance, $d(x) = 4.0(x - 0.625)$

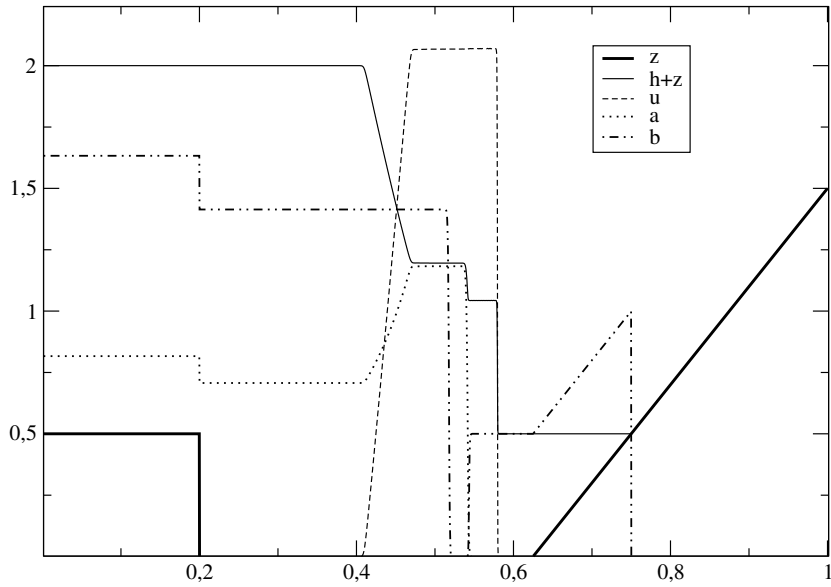


Figure 4: Reference solution at time $t = 0.02$ computed at second order with 3300 points

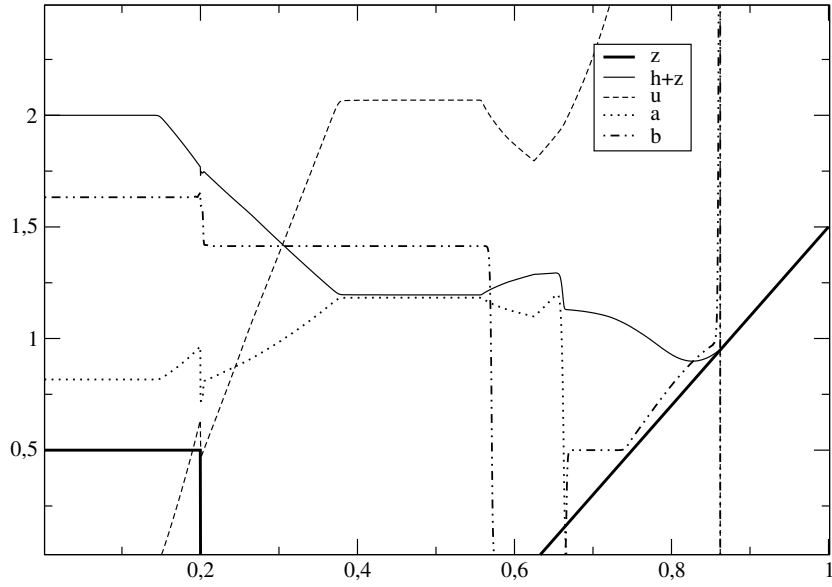


Figure 5: Reference solution at time $t = 0.08$ computed at second order with 3300 points

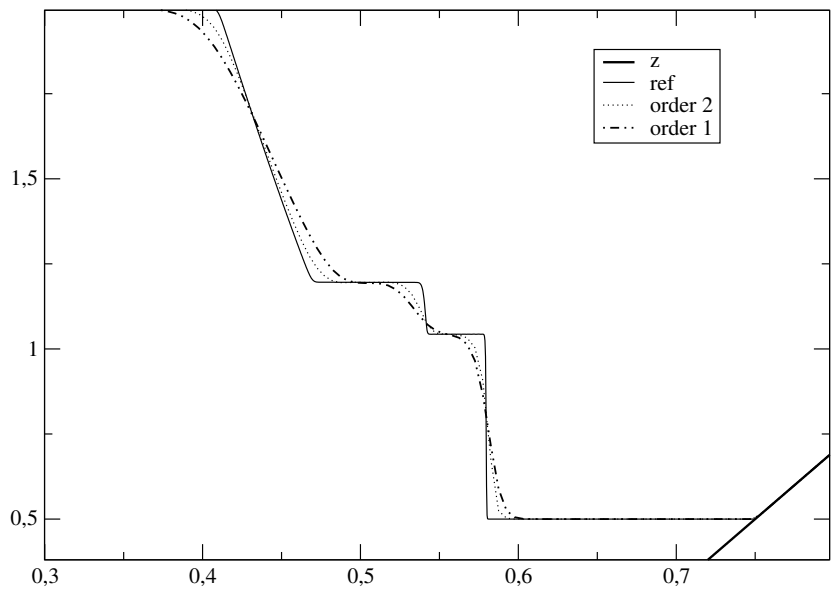


Figure 6: Solution $h + z$ at time $t = 0.02$ computed at first and second order with 200 points. The reference solution is the continuous line.

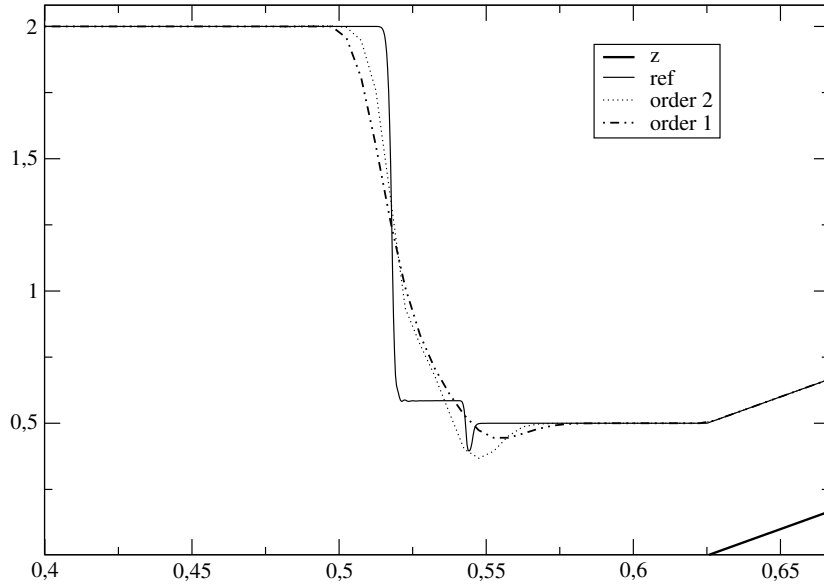


Figure 7: Solution v at time $t = 0.02$ computed at first and second order with 200 points. The reference solution is the continuous line.

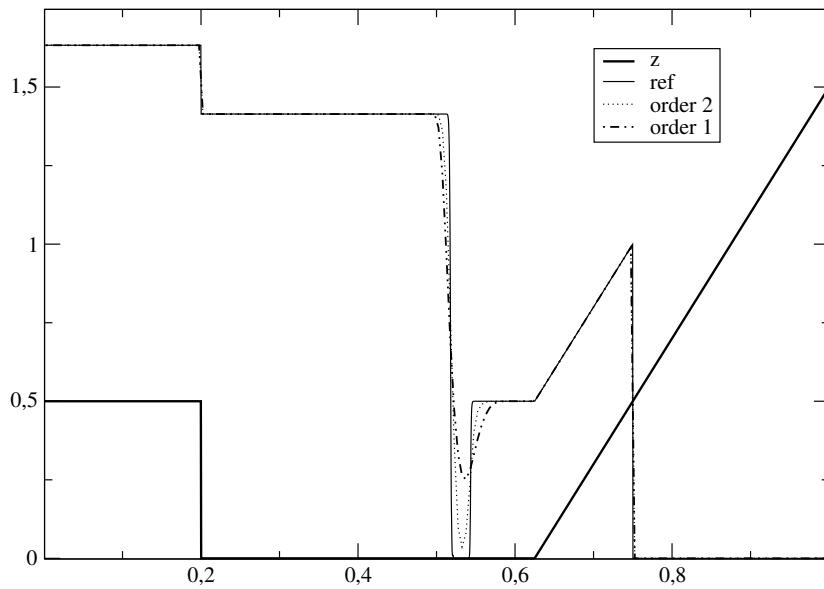


Figure 8: Solution b at time $t = 0.02$ computed at first and second order with 200 points. The reference solution is the continuous line.

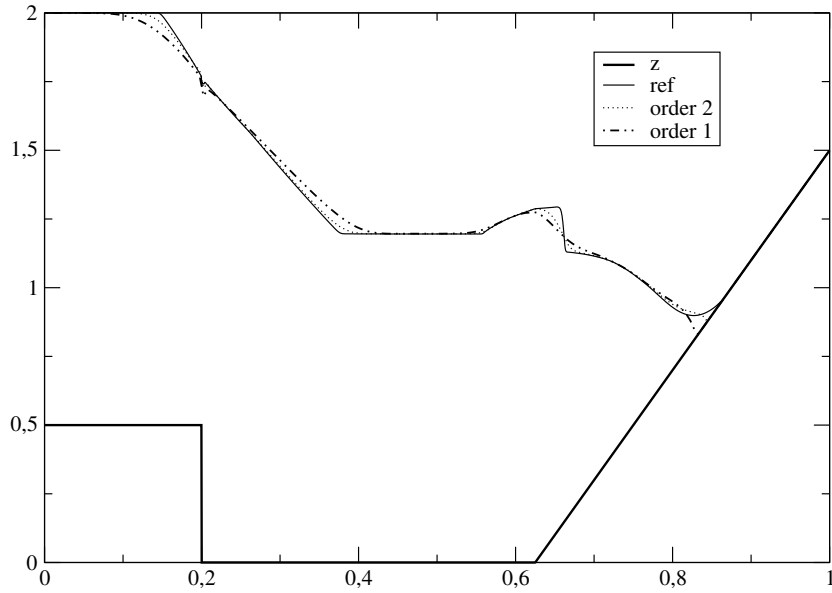


Figure 9: Solution $h + z$ at time $t = 0.08$ computed at first and second order with 200 points. The reference solution is the continuous line.

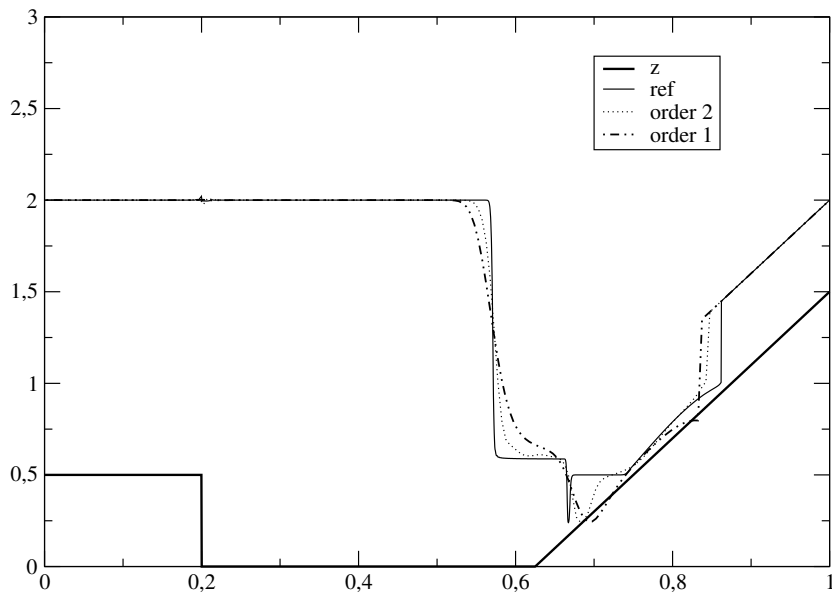


Figure 10: Solution v at time $t = 0.08$ computed at first and second order with 200 points. The reference solution is the continuous line.

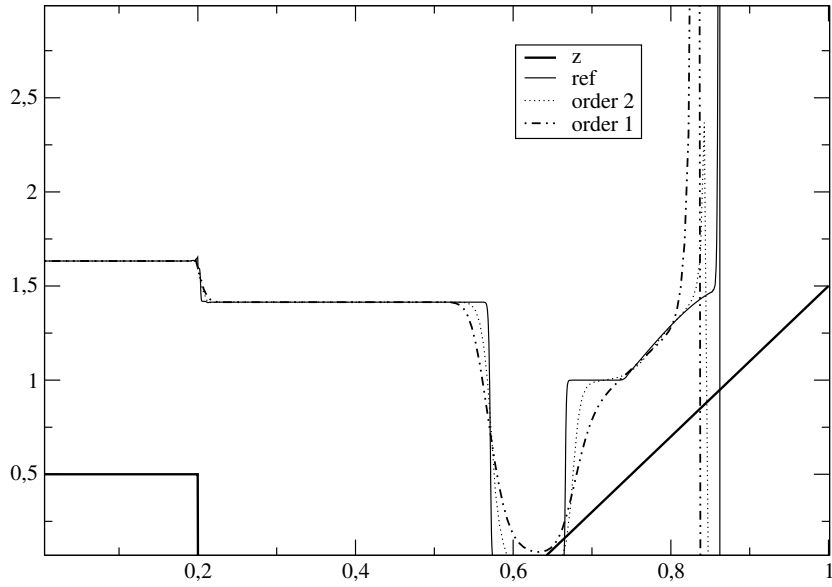


Figure 11: Solution b at time $t = 0.08$ computed at first and second order with 200 points. The reference solution is the continuous line.

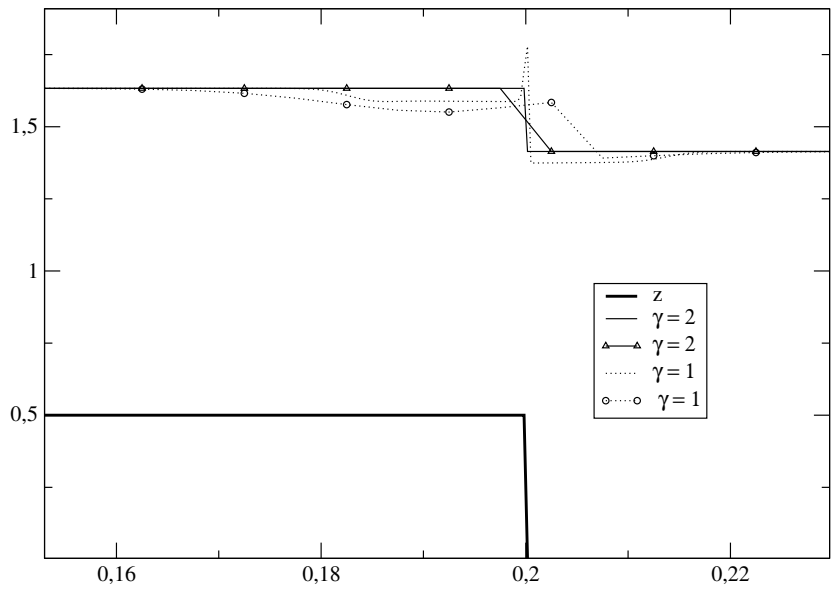


Figure 12: Solution b at time $t = 0.02$ computed at first order with 200 points with different values of γ . The reference solutions are the continuous lines.

References

- [1] E. Audusse, F. Bouchut, M.-O. Bristeau, R. Klein, B. Perthame, *A fast and stable well-balanced scheme with hydrostatic reconstruction for shallow water flows*, SIAM J. Sci. Comp. 25 (2004), 2050-2065.
- [2] D.S. Bale, R.J. Leveque, S. Mitran, J.A. Rossmanith, *A wave propagation method for conservation laws and balance laws with spatially varying flux functions*, SIAM J. Sci. Comput. 24 (2002), 955-978.
- [3] C. Berthon, F. Foucher, *Efficient well-balanced hydrostatic upwind schemes for shallow water equations*, J. Comput. Phys. 231 (2012), 4993-5015.
- [4] C. Chalons, F. Coquel, E. Godlewski, P.-A. Raviart, N. Seguin, *Godunov-type schemes for hyperbolic systems with parameter-dependent source. The case of Euler system with friction*, Math. Models Methods Appl. Sci. 20 (2010), 2109-2166.
- [5] D.S. Balsara, M. Dumbser, R. Abgrall, *Multidimensional HLL and HLLC Riemann solvers for unstructured meshes with application to Euler and MHD flows*, J. Comput. Phys. 261 (2014), 172-208.
- [6] F. Bouchut, *Nonlinear stability of finite volume methods for hyperbolic conservation laws, and well-balanced schemes for sources*, Birkhäuser, 2004.
- [7] F. Bouchut, S. Boyaval, *A new model for shallow viscoelastic fluids*, Math. Models and Meth. in Appl. Sci. 23 (2013), 1479-1526.
- [8] F. Bouchut, X. Lhébrard, *A 5-wave relaxation solver for the shallow water MHD system*, 2015.
- [9] F. Bouchut, C. Lusso, V. Zeitlin, *Geostrophic vs magnetostrophic adjustment and nonlinear magneto-inertia-gravity waves in rotating shallow water magnetohydrodynamics*, 2014.
- [10] F. Bouchut, T. Morales, *A subsonic-well-balanced reconstruction scheme for shallow water flows*, Siam J. Numer. Anal. 48 (2010), 1733-1758.
- [11] F. Bouchut, V. Zeitlin, *A robust well-balanced scheme for multi-layer shallow water equations*, Discrete and Continuous Dynamical Systems B, 13 (2010), 739-758.
- [12] M.J. Castro, E.D. Fernández-Nieto, *A class of computationally fast first order finite volume solvers: PVM methods*, SIAM J. Sci. Comput. 34 (2012), 2173-2196.
- [13] M.J. Castro, A. Pardo, C. Parés, *Well-balanced numerical schemes based on a generalized hydrostatic reconstruction technique*, Math. Models Methods Appl. Sci. 17 (2007), 2065-2113.
- [14] M.J. Castro, A. Pardo, C. Parés, E.F. Toro, *On some fast well-balanced first order solvers for nonconservative systems*, Math. Comput. 79 (2010), 1427-1472.

- [15] A. Chertock, A. Kurganov, Y. Liu, *Central-upwind schemes for the system of shallow water equations with horizontal temperature gradients*, Num. Math. 127 (2014), 595-639.
- [16] P.J. Dellar, *Hamiltonian and symmetric hyperbolic structures of shallow water magnetohydrodynamics*, Physics of Plasmas 9 (2002), 1130.
- [17] H. DeSterck, *Hyperbolic theory of the shallow water magnetohydrodynamics equations*, Physics of Plasmas 8 (2001), 3293.
- [18] F.G. Fuchs, A.D. McMurry, S. Mishra, N.H. Risebro, K. Waagan, *Approximate Riemann solvers and robust high-order finite volume schemes for multi-dimensional ideal MHD equations*, Comm. Comput. Phys. 9 (2011), 324-362.
- [19] D.L. George, *Augmented Riemann solvers for the shallow water equations over variable topography with steady states and inundation*, J. Comput. Phys. 227 (2008), 3089-3113.
- [20] P.A. Gilman, *Magnetohydrodynamic "shallow water" equations for the solar tachocline*, Astrophys. J. Lett. 544 (2000), L79-L82.
- [21] C. Parés, *Numerical methods for nonconservative hyperbolic systems: a theoretical framework*, SIAM J. Numer. Anal. 44 (2006), 300-321.
- [22] C. Parés, M. Castro, *On the well-balance property of Roe's method for nonconservative hyperbolic systems. Applications to shallow-water systems*, Math. Modelling Num. Anal. 38 (2004), 821-852.
- [23] S. Qamar, G. Warnecke, *Application of space-time CE/SE method to shallow water magnetohydrodynamic equations*, J. Comput. Appl. Math. 196 (2006), 132-149.
- [24] J.A. Rossmannith, *A constrained transport method for the shallow water MHD equations*, in Hyperbolic problems: theory, numerics, applications, 9th International Conference on Hyperbolic Problems, Pasadena, 2002, Ed. T.Y. Hou, E. Tadmor, 851-860, 2003.
- [25] J.A. Rossmannith, D.S. Bale, R.J. Leveque, *A wave propagation algorithm for hyperbolic systems on curved manifolds*, J. Comput. Phys. 199 (2004), 631-662.
- [26] Y. Xing, C.-W. Shu, *A survey of high order schemes for the shallow water equations*, J. Math. Study 47 (2014), 221-249.
- [27] V. Zeitlin, *Remarks on rotating shallow-water magnetohydrodynamics*, Non-linear Processes in Geophysics 20 (2013), 893-898.